ELSEVIER

NeuroImage

www.elsevier.com/locate/ynimg
NeuroImage 31 (2006) 1536 – 1548

Separating respiratory-variation-related fluctuations from neuronal-activity-related fluctuations in fMRI

Rasmus M. Birn,* Jason B. Diamond, Monica A. Smith, and Peter A. Bandettini

Laboratory of Brain and Cognition, National Institute of Mental Health, NIH, 10 Center Dr., Bldg. 10, Rm. 1D80 Bethesda, MD 20892-1148, USA

Received 26 August 2005; revised 9 January 2006; accepted 16 February 2006
Available online 24 April 2006

Subtle changes in a subject's breathing rate or depth, which occur naturally during rest at low frequencies (<0.1 Hz), have been shown to be significantly correlated with fMRI signal changes throughout gray matter and near large vessels. The goal of this study was to investigate the impact of these low-frequency respiration variations on both task activation fMRI studies and resting-state functional connectivity analysis. Unlike MR signal changes correlated with the breathing motion (~0.3 Hz), BOLD signal changes correlated with across-breath variations in respiratory volume (~0.03 Hz) appear localized to blood vessels and regions with high blood volume, such as gray matter, similar to changes seen in response to a breath-hold challenge. In addition, the respiration-variation-induced signal changes were found to coincide with many of the areas identified as part of the 'default mode' network, a set of brain regions hypothesized to be more active at rest. Regions could therefore be classified as being part of a resting network based on their similar respiration-induced changes rather than their synchronized neuronal activity. Monitoring and removing these respiration variations led to a significant improvement in the identification of task-related activation and deactivation and only slight differences in regions correlated with the posterior cingulate at rest. Regressing out global signal changes or cueing the subject to breathe at a constant rate and depth resulted in an improved spatial overlap between deactivations and resting-state correlations among areas that showed deactivation.
Published by Elsevier Inc.

Introduction

The central challenge in functional magnetic resonance imaging (fMRI) is the detection of relatively small neuronal-activation-induced blood oxygenation changes in the presence of various other signal fluctuations. In addition to thermal noise, scanner related variations, and bulk subject movement, signal fluctuations can be caused by several physiological processes. Pulsations of the blood induced by the heart beat, for example, result in signal changes mostly in voxels containing a high proportion of blood and/or cerebral spinal fluid (CSF). In addition, movement of the chest during respiration causes magnetic field changes that can cause a shifting of the brain image. Respiration can affect the fMRI time series in another way—by changing the arterial level of CO_2, a potent vasodilator. This is perhaps most clearly seen in response to a breath-holding challenge, where a breath-hold of 30 s duration results in an average signal increase of 3–5% (Kastrup et al., 1999a,b,c; Li et al., 1999; Stillman et al., 1995). More recently, studies have shown that small fluctuations in end-tidal CO_2 at a frequency of about 0.03 Hz occur naturally during normal breathing at rest and are significantly correlated with the blood-oxygenation-level-dependent (BOLD) fMRI signal fluctuations (Wise et al., 2004). These CO_2 fluctuations are hypothesized to be due to subtle changes in the depth and rate of breathing during the scan. Existing physiologic correction techniques reduce MR signal changes occurring in synchrony with the respiratory cycle, corresponding to the movement associated with respiration, but they do not correct for variations in the inspired volume. This, of course, raises the concern that changes in breathing patterns during an fMRI experiment, which may be task or stimulus correlated, may lead to artifactual signal changes or mask existing function. Determining the impact of these fluctuations on fMRI studies and developing methods to correct for these variations are therefore of critical importance.

Low-frequency fluctuations induced by changes in breathing are particularly problematic for resting-state functional connectivity analysis, a technique that infers the connections of neuronal networks by measuring the correlation of low-frequency (<0.1 Hz) BOLD-fMRI signal fluctuations between and within brain regions (Biswal et al., 1995; Lowe et al., 1998). These low-frequency BOLD fluctuations are hypothesized to result from oscillations in neuronal activity synchronized within and across brain regions. There are, however, other factors that can cause signals in different parts of the brain to be correlated. Cardiac pulsations are often present and synchronized in regions of high blood volume or CSF. Respiration fluctuations often appear near edges in the image. Techniques have therefore been implemented to remove fluctua-

* Corresponding author. Fax: +1 301 402 1370.
E-mail address: rbirn@nih.gov (R.M. Birn).
Available online on ScienceDirect (www.sciencedirect.com).

1053-8119/$ - see front matter. Published by Elsevier Inc.
doi:10.1016/j.neuroimage.2006.02.048

tions at these cardiac and respiration frequencies (and their harmonics) prior to the functional connectivity analysis (Biswal et al., 1996; Chuang and Chen, 2001; Glover et al., 2000; Hu et al., 1995). The variations in respiration depth from breath to breath, however, occur at much lower frequencies which are not filtered out by typical physiological correction routines. Furthermore, the frequency of these respiratory changes (~0.03 Hz) overlaps with the frequencies of fluctuations believed to result from varying brain activity at rest (<0.1 Hz). Therefore, there is still the danger that the functional network identified by this correlation method in fact represents areas where the fMRI signal has similar respiratory-change-related fluctuations, such as large vessels.

The goals of this study were: (1) to characterize the temporal and spatial patterns of respiration-variation-induced fMRI signal changes; (2) to investigate the impact of these respiration fluctuations on fMRI time series, both for task-related activation and for resting-state functional connectivity analysis; and (3) to evaluate potential methods to reduce this artifact. A method is presented by which these variations in respiration can be estimated from a respiration belt placed around the subject's chest without the need for a separate monitor for end-tidal CO_2. The paradigm used in this study was a lexical decision task. In addition to activations in motor and language areas, this task commonly results in deactivations in the anterior and posterior cingulate. Such deactivations are observed across a wide range of tasks and are believed to reflect brain regions that are more active during rest, therefore referred to as the "default mode network" (Raichle et al., 2001). Recently, Greicius et al. showed that brain regions within this default mode network are also correlated at rest, supporting the notion that the default mode network reflects the activity of the brain when not performing a specific cognitive task (Greicius et al., 2003). We chose to use this system to investigate the impact of respiration changes on resting-state functional connectivity analysis for two primary reasons. First, the deactivations can define a starting point for determining which brain regions are correlated. Secondly, the regions within the default mode network overlap with many of the regions that are strongly affected by respiration changes (i.e. where the fMRI signal is significantly correlated with fluctuations in end-tidal CO_2). While there may indeed be true differences between task-related deactivations and resting-state connectivity in the default mode network, our hypothesis is that the additional respiration fluctuations lead to errors in defining the network of neurons correlated during rest and that reducing the variability of breathing or regressing out these fluctuations leads to an improved ability to detect function and a better agreement between deactivations and regions correlated with these areas at rest.

Methods

Subjects and imaging parameters

Ten normal, healthy, right-handed volunteers were scanned under an Institutional Review Board (IRB) approved protocol after obtaining informed consent. Time series of T2*-weighted echo-planar MR images were acquired on a 3 T General Electric (GE) Signa MRI scanner (Waukesha, WI, USA) using an 8-channel GE receive coil with whole body RF excitation. Whole brain coverage was achieved using 27–28 sagittal 5 mm thick slices (TR: 2000 ms, TE: 30 ms, FOV: 24 cm, slice thickness: 5 mm, matrix: 64 × 64, 165 image volumes per time series.)

Tasks

In two time series, subjects performed a lexical decision task, where either words or "non-words" were presented visually, and the subject's response (word or non-word) was recorded using a button press. The task was presented in a blocked design (30-s task blocks alternated with 30 s of rest) with words or non-words presented every 2 s during the task block. Additional time series consisted of subjects either resting with their eyes closed ('Rest') or resting while regulating their breathing by following a visual stimulus that oscillated at a constant rate ('Constant Respiration'). The rate of this constant breathing was chosen to be equal to the subject's average breathing rate during the normal resting time series (~15–20 breaths/min). Each of these resting time series was performed twice in 8 of the 10 subjects. For the other 2 subjects, there was insufficient time to repeat the resting run. A subset of 8 subjects also performed a breath-holding task consisting of a 20-s breath-hold at the end of expiration alternated with 40 s of normal breathing. This breath-hold cycle was repeated four times in a run (beginning and ending the run with normal breathing) for a total of 280 s.

Physiological monitoring

Subjects' heart beats were recorded using a pulse-oximeter placed on the left index finger. These pulse-oximeter waveforms were used to determine the phase of the cardiac cycle in which each MR image was acquired. Respiration was measured with a pneumatic belt positioned at the level of the abdomen. The amount of air inspired with each breath was estimated by computing the difference between the maximum and minimum belt positions at the peaks of inspiration and expiration, respectively. This difference was divided by the period of the respiration (i.e. the time between the peaks of the respiration waveform) in order to take into account changes in the rate, in addition to the depth, of breathing. This estimate was interpolated to even multiples of the imaging TR so that it could be used as a regressor in the fMRI time series analysis and is an estimate of the respiration volume per time (RVT).

Analysis

All image analysis was performed using AFNI (Cox, 1996). Reconstructed images were first corrected for motion using a rigid-body volume registration. Functional activation maps were computed from the lexical task by correlating each voxel's fMRI response time course with an ideal response function consisting of a Gamma-variate function convolved with the blocked design stimulus timing. To evaluate the effects of different physiologic corrections, the regression was performed in three ways: (1) without physiologic correction; (2) with a modified version of a conventional physiologic correction routine, RETROICOR (Glover et al., 2000); and (3) with the modified RETROICOR and an additional regressor to model the respiratory volume per time (computed as described above) ('Respiration volume per time correction', or 'RVTcor'). In the modified RETROICOR routine, additional regressors corresponding to the oscillations at the cardiac (~1 Hz) and respiratory (~0.3 Hz) frequency and their first harmonics were formed (as described in Glover et al. (2000)) and used together with the ideal BOLD response to the lexical task in a multiple regression analysis. This is equivalent to the

'Nuisance Variable Regression' (NVR) method proposed by Lund et al. (2006) for the removal of physiological noise and other regressors of no interest. For the respiration volume per time correction, the regression was computed with the 8 physiological regressors used in the RETROICOR correction and an additional regressor that represents the respiration volume per time, computed from the respiration belt measurement. This regression was repeated for 51 shifts of the respiration volume per time regressor (from −10 s to +15 s, in ½-s increments) in order to account for the unknown and likely variable delay between the respiration changes and the fMRI signal change. Each regression included only one shift of the respiration volume per time estimate with that shift corresponding to the latency of the BOLD response to the estimate. The correlation at negative shifts of the respiration measure relative to the fMRI signal was assessed to look for possible feedback effects. That is, in addition to respiration changes causing changes in blood flow and fMRI signals, the level of CO_2 in the blood (which is reflected in the blood flow and fMRI signal) could stimulate chemoreceptors that lead to subsequent changes in respiration. For each voxel, the largest Z score of detecting the BOLD response to the lexical task from the 51 regressions was chosen as the "best" correction (RVTcor). (For deactivations, this was the largest negative Z score.)

Average Z scores from the lexical task for each subject were computed for a fixed region of interest, defined as the voxels which were considered "active" (i.e. correlated with the canonical task-related BOLD response with a Z score greater than 5.32 ($P < 10^{-7}$ uncorrected)) for all three processing schemes (no correction, RETROICOR, and RVTcor). These ROI-averaged Z scores were averaged across all 10 subjects to obtain a measure of the impact of the different correction schemes.

The improvements afforded by the different physiological corrections and by constant breathing were also evaluated by comparing the standard deviation of the MR signal over time. To eliminate the potential confound of increased variance in regions of task-related activation, this standard deviation measurement was performed on runs where the subjects were at rest, with either normal or constant respirations and following the two different correction routines. In this case, the correction consisted of regressing out the relevant physiological variations (i.e. the residuals of a regression analysis) rather than including these variations as additional regressors in the analysis to detect function. For RVTcor, the 51 different regressions were combined by choosing for each voxel the regression (i.e. the latency of the respiration volume per time estimate) that resulted in the maximal negative correlation between the respiration volume per time estimate and the fMRI signal.

Group maps of regions affected by respiration volume per time changes were computed by averaging the Z scores of the correlation of the respiration volume per time with the resting time course in all 10 subjects. One run was discarded due to excessive subject motion, and another was discarded due to a failure of the respiration belt measurement for that run. A second measure to reflect the likelihood that a given region is significantly affected by respiration was obtained by first creating for each subject, for each of the resting and lexical runs, a mask consisting of those voxels significantly correlated with respiration volume per time (CC > 0.4, $P < 10^{-6}$ uncorrected). These masks were transformed to Talairach coordinates, smoothed with a Gaussian blur with a full-width at half maximum of 2 mm, and averaged across all resting and lexical runs from 10 subjects. The resulting mean reflects the fraction of runs in which a particular voxel was significantly correlated with the changes in respiration.

In a recent study by Fox et al., improvements in resting-state correlation maps were obtained by removing signal changes that are similar in time over the entire brain (the "global" signal) (Fox et al., 2005). A measure of the global signal change over time was obtained by averaging in each subject and for each resting run the time courses over the whole brain. This global brain signal was compared with changes in respiration, as measured from the respiration belt. In addition, the global signal was correlated with the resting time course, and the residual of this regression was used for further functional connectivity analysis.

In the subset of 8 subjects that performed a breath-holding task, changes in respiration volume were modeled using an inverted boxcar waveform, with decreases during periods of breath-holding. The location and amplitude of breath-hold-induced fMRI signal changes were obtained in a similar manner as the analysis of resting variations in respiration. The correlation between the respiration volume per time (in this case an inverted boxcar) and the fMRI signal was computed at 51 different shifts of the boxcar (in 1-s increments, from −10 s to +40 s). These 51 correlation maps were combined by choosing for each voxel the shift that resulted in the maximal negative correlation. This corresponds to an increase in the fMRI signal in response to breath-holding.

Functional connectivity analyses were performed on the resting-state data with and without physiologic corrections, after regressing out global signal changes, and for both breathing conditions (normal and constant). This analysis consisted of first defining, for each subject, a region of interest based on the intersection of voxels in the posterior cingulate (as defined by the Talairach Daemon (UTHSCSA, San Antonio, TX, http://ric.uthscsa.edu/projects/talairachdaemon.html)) and voxels that showed a deactivation during the lexical decision task. The signal intensity time courses during rest from voxels within this ROI were averaged and correlated with the resting time courses each voxel in the brain. This correlation analysis is similar to that performed by previous investigations into resting-state networks (Biswal et al., 1995; Greicius et al., 2003; Lowe et al., 1998).

The resting-state correlations can also be computed by correlating the data from each of the voxels in the defined ROI with every other voxel time series in the brain, forming a series of correlation maps which could then be averaged. This analysis would allow for differences in the latency of the BOLD fluctuations within the ROI. In this particular study, however, no significant difference in latency of the BOLD response was found in voxels located within the posterior cingulated. The results of this analysis were therefore identical to correlating with an averaged ROI time course and were therefore not evaluated further.

Results

Cardiac fluctuations were most prominent in regions with CSF and with large vessels, such as the sagittal sinus and the Circle of Willis. Signal changes correlated with the respiration-related chest movement at 0.3 Hz were minimal and primarily located at the edges of the image in the phase encoding direction, consistent with a magnetic field shift in synchrony with the chest movement. The depth of breathing (divided by the breath-to-breath period) varied on average by about 28.1% ± 11.8% (computed as the standard deviation of the RVT measure across time) at a frequency of

approximately 0.03 Hz during rest (see Fig. 1A). These variations were typically more pronounced for resting runs compared to task runs. Respiration depth during the lexical task varied by 19.1% ± 8.6%. When subjects were cued to breathe at a constant rate and depth, respiration depth varied by 17.9% ± 4.2%. These respiration changes were significantly correlated with fMRI signal changes, particularly in highly vascular regions, such as gray matter and large vessels (see Fig. 2). In the posterior cingulate, 76% of resting and lexical runs (i.e. time series without an explicit modulation of respiration) were significantly correlated with respiration changes, while in the inferior occipital cortex, up to 90% of the resting and lexical runs were significantly correlated. This correlation was predominantly negative, with fMRI signal increases resulting from decreases in respiration depth, at an average latency of 5.4 s (averaged over voxels negatively correlated with the respiration volume per time with a significance of $Z < -5.4$, $P < 10^{-7}$ uncorrected). This latency varied for different voxels across the brain. In addition, a positive correlation was observed when the respiration volume per time was shifted on average by −0.9 s relative to the fMRI signal (averaged over voxels significantly positively correlated with the respiration volume per time). Each voxel that was correlated with the respiration volume per time showed both a positive and a negative correlation at different latencies, with the positive correlation preceding the negative by an

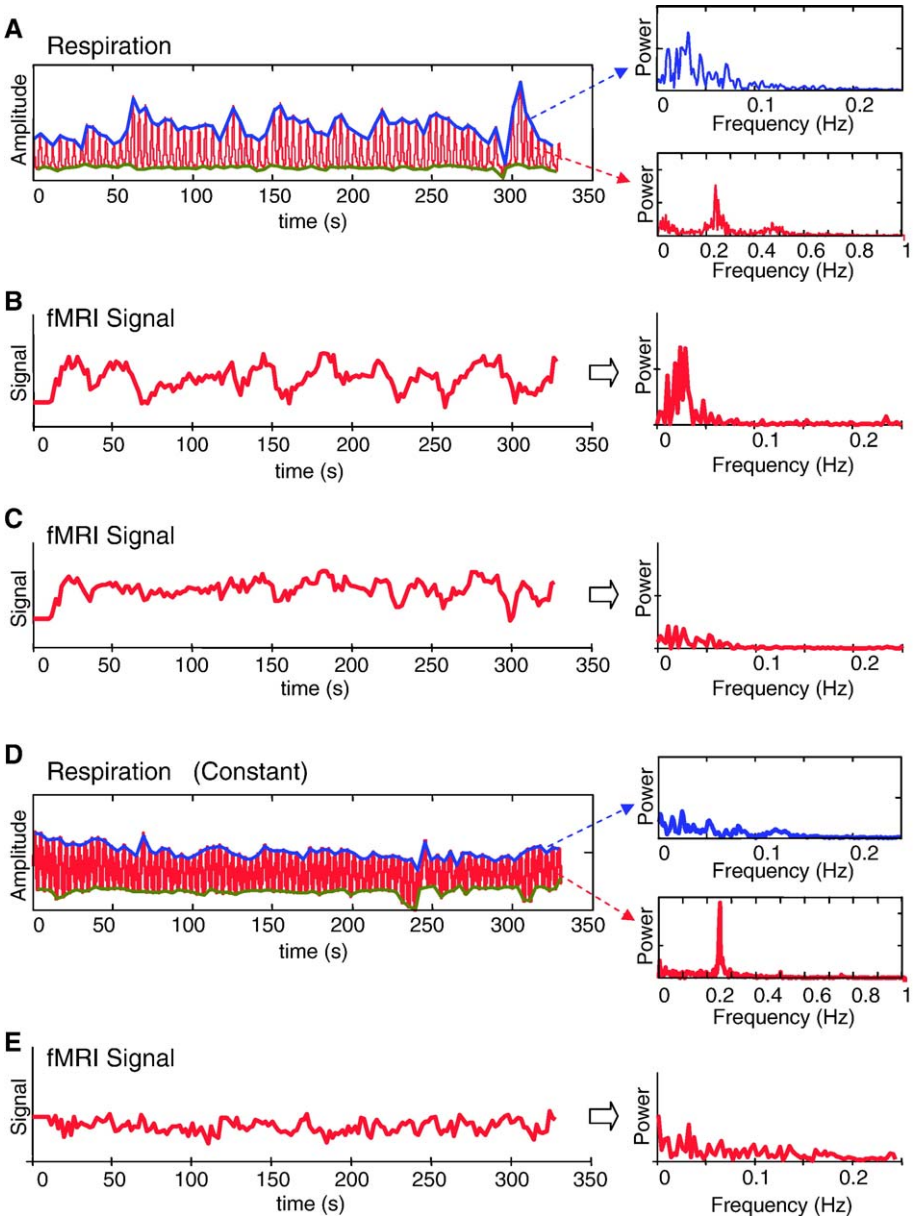

Fig. 1. Time courses: (A) an example of respirations measured from the respiration belt around the subject's abdomen. Graphs on the right show the Fourier transform of the respiration (red) and the respiration volume per time (RVT) (blue) derived from the envelope, or breath-to-breath variability, of the respiration depth and rate. (B) fMRI signal in a voxel correlated with respiration volume changes. (C) fMRI signal in the same voxel after regressing out respiration volume per time changes. (D) Respirations and Fourier transforms of respiration and RVT when subject was cued to breathe at a constant depth and rate. (E) fMRI signal in the same voxel as shown in panels B and C, but during constant respirations.

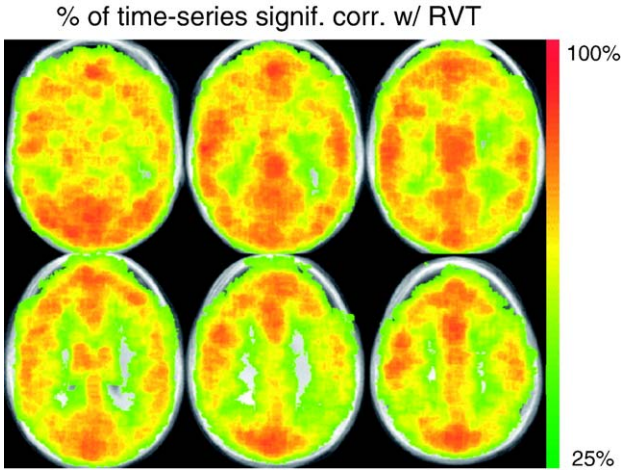

Fig. 2. Location of respiration changes: map showing for each voxel the percentage of time series (out of a total of 16 runs from 10 subjects) where the fMRI signal during rest was significantly (CC > 0.4, $P < 10^{-6}$ uncorrected) correlated with the respiration volume per time (RVT) changes. Signal changes are largest in gray matter and near large blood vessels.

average of 10.3 s (see Fig. 3). (The reason that this value is larger than the difference between the average latencies for the negative and positive correlations (5.4 s and −0.9 s, respectively) is that this value reports the average difference *within* each voxel, whereas the significant positive or negative correlations were averaged over different voxel pools.) Global fMRI signal changes during rest were significantly correlated with changes in respiration volume per time (CC = −0.50 ± 0.13) at a latency of 8.8 s ± 2.6 s. This correlation and latency refer to the maximum negative correlation between the global fMRI time course and the respiration volume per time evaluated at 51 shifts from −10 s to +15 s. When the global signal was correlated with the fMRI data, the resultant maps were similar to maps of regions significantly correlated with respiration volume per time changes.

The standard deviation of the fMRI signal over time was greatest in gray matter and in regions corresponding to larger vessels (see Fig. 4). The average temporal standard deviation over the whole brain was 1.41%, with fluctuations as high as 10% in vascular regions. These variations were reduced when the RETROICOR correction was applied (from 1.41% to 1.29%, averaged over all subjects) and further reduced when the respiration volume per time was modeled (from 1.29% to 1.20%) (see Fig. 5). Again, the largest improvement is seen in regions corresponding to large vessels. While the temporal noise was reduced by different amounts in different parts of the brain, in no part of the brain was the standard deviation increased when the additional respiration volume per time regressor was added. Only decreases in the noise were observed. When the subject breathed at a constant rate, the variation over time was reduced from 1.41% to 1.25%. This was further improved by the RETROICOR correction, reducing the temporal variation to 1.08%.

The lexical decision task resulted in activations in the left and right precentral gyrus, middle occipital gyrus, fusiform gyrus, and inferior frontal gyrus. Decreases in the fMRI signal during task performance were observed in the anterior cingulate, posterior cingulate, precuneus, and the superior occipital gyrus (see Figs. 6A and 7A). These regions have previously been implicated as part of a 'default mode' network—a set of brain regions generally active during rest and "deactivated" for cognitively demanding tasks (Greicius et al., 2003; Raichle et al., 2001). An unthresholded Z score maps of these activations are shown in Fig. 8.

When corrections for fluctuations synchronous with the cardiac and respiratory cycle (RETROICOR) were applied, the Z scores for detecting signal changes correlated with the expected blocked design BOLD response increased on average by approximately 1% (from 7.8 to 7.9). This average was computed in each subject over all voxels significantly active (or deactive) at a Z score > 5.3 (or <−5.3), $P < 10^{-7}$ uncorrected. When the respiration volume per time was used as an additional regressor, the Z scores improved on average by an additional 8% (from 7.9 to 8.5). This improvement was greatest in activations that were near large vessels (see Fig. 9).

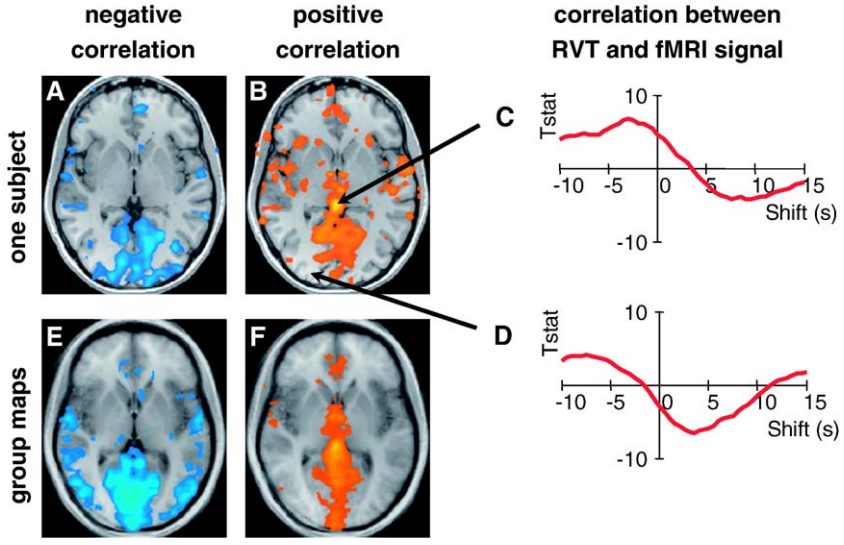

Fig. 3. Correlation with respiration volume per time: (A) Z scores of regions negatively correlated with the respiration volume per time (RVT) in one subject; (B) regions positively correlated with the RVT in one subject. (C and D) Z score of correlating the RVT with fMRI time course (for two sample voxels, as indicated by the arrows) at multiple shifts between the RVT and the time series. Positive shifts indicate a shift of the RVT forward in time relative to the fMRI data (i.e. fMRI signal changes following respiration changes). (E and F) Similar maps as shown in panels A and B but averaged over 10 subjects.

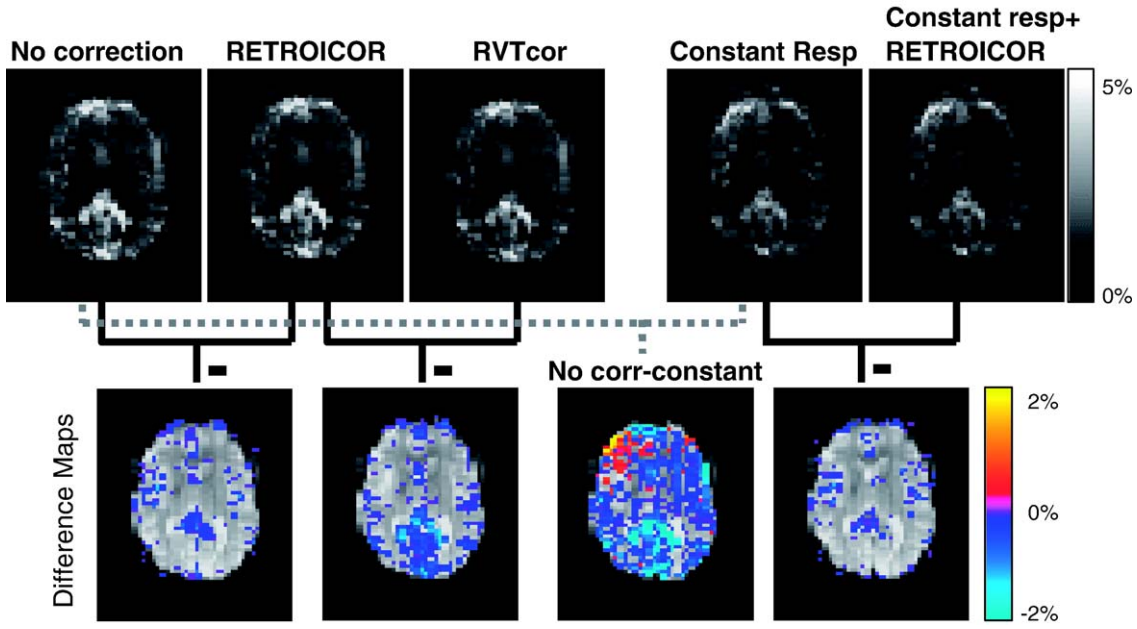

Fig. 4. Standard deviation maps: maps of temporal standard deviation for five conditions—no correction, correction using RETROICOR, respiration volume per time correction (RVTcor), constant respirations, and constant respirations with RETROICOR. These maps are from one resting run in one representative subject. Difference maps highlight the reduction in standard deviation for each correction step.

The significance of detecting deactivations was also increased substantially by the respiration volume per time correction.

During rest, fMRI signal changes in the posterior cingulate were significantly correlated with signal fluctuations in the anterior cingulate, superior occipital, and inferior parietal gyri—regions that were deactivated during the lexical task. In addition, there was correlation with a number of other regions not deactivated in the lexical task, including a large region in the inferior occipital gyrus (see Figs. 6C and 7C). Many of these latter regions were significantly correlated with changes in respiration volume per time. When fMRI signal fluctuations correlated with changes in respiration volume per time were regressed out, correlations between the posterior cingulate and these additional areas were slightly reduced, but were still present (see Figs. 6D and 7D). When respirations were held at a more constant rate and depth, correlation of these additional regions with the posterior cingulate at rest was reduced, and the "functionally correlated" network included only those regions that were deactivated during the lexical task (see Figs. 6E and 7E). A similar change is seen when the global signal is regressed out of each voxel's resting-state time course prior to the connectivity analysis (see Figs. 6F and 7F). Regions correlated with the average signal from deactivated voxels in the posterior cingulate include predominantly those other regions that were deactivated during the lexical task, and fewer regions that were not deactivated but strongly correlated with respiration changes. These differences are not purely due to differences in the statistical threshold, as can be seen on unthresholded Z score maps shown in Fig. 8.

In the 8 subjects performing the breath-holding task, the fMRI signal increased significantly following a 20-s period of breath-holding. In agreement with earlier breath-holding studies, these changes were most pronounced in gray matter and veins, with signal changes up to 10%, and an average signal change over the whole brain of 2.8%. There are strong similarities between the relative amplitudes of breath-holding-induced fMRI signal change across the brain compared to the relative amplitude of signal changes correlated with variations in respiration depth during rest (see Fig. 10). A scatter plot showing the correlation of these two measures for all the voxels in this subject's brain (CC = 0.76) is shown in Fig. 11. While there is good correlation between breath-hold-induced changes and signal variations correlated with RVT at rest, the changes during rest appear more localized, with regions in

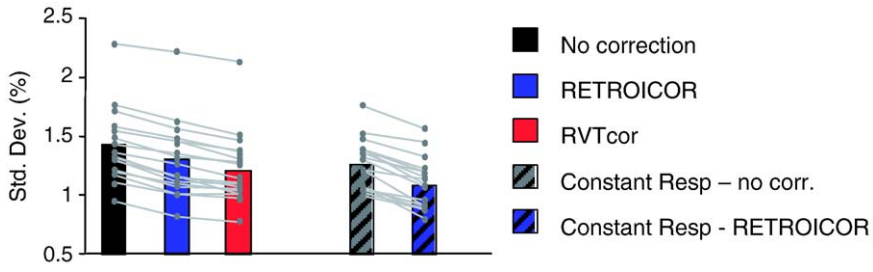

Fig. 5. Standard deviation: average temporal standard deviation without correction, with RETROICOR correction, respiration volume per time correction (RVTcor), constant respirations, and constant respirations with RETROICOR. Lines indicate temporal standard deviation for each subject, averaged over the whole brain. Bar graph indicates average over all subjects.

the occipital cortex, for example, showing relatively greater activation compared to other brain regions.

Discussion

There is a growing interest in low-frequency fluctuations of the fMRI signal at rest, driven by the theory that these fluctuations reflect variations in brain activity during rest. Biswal and colleagues, for example, first noticed correlations in low-frequency fMRI signal fluctuations between the left and right motor cortices even when subjects were not explicitly performing a motor task (Biswal et al., 1995). Since then, studies have shown correlated fMRI signals in a number of other systems when no explicit task was being performed, including the auditory system, visual system, and language areas, in addition to areas commonly showing

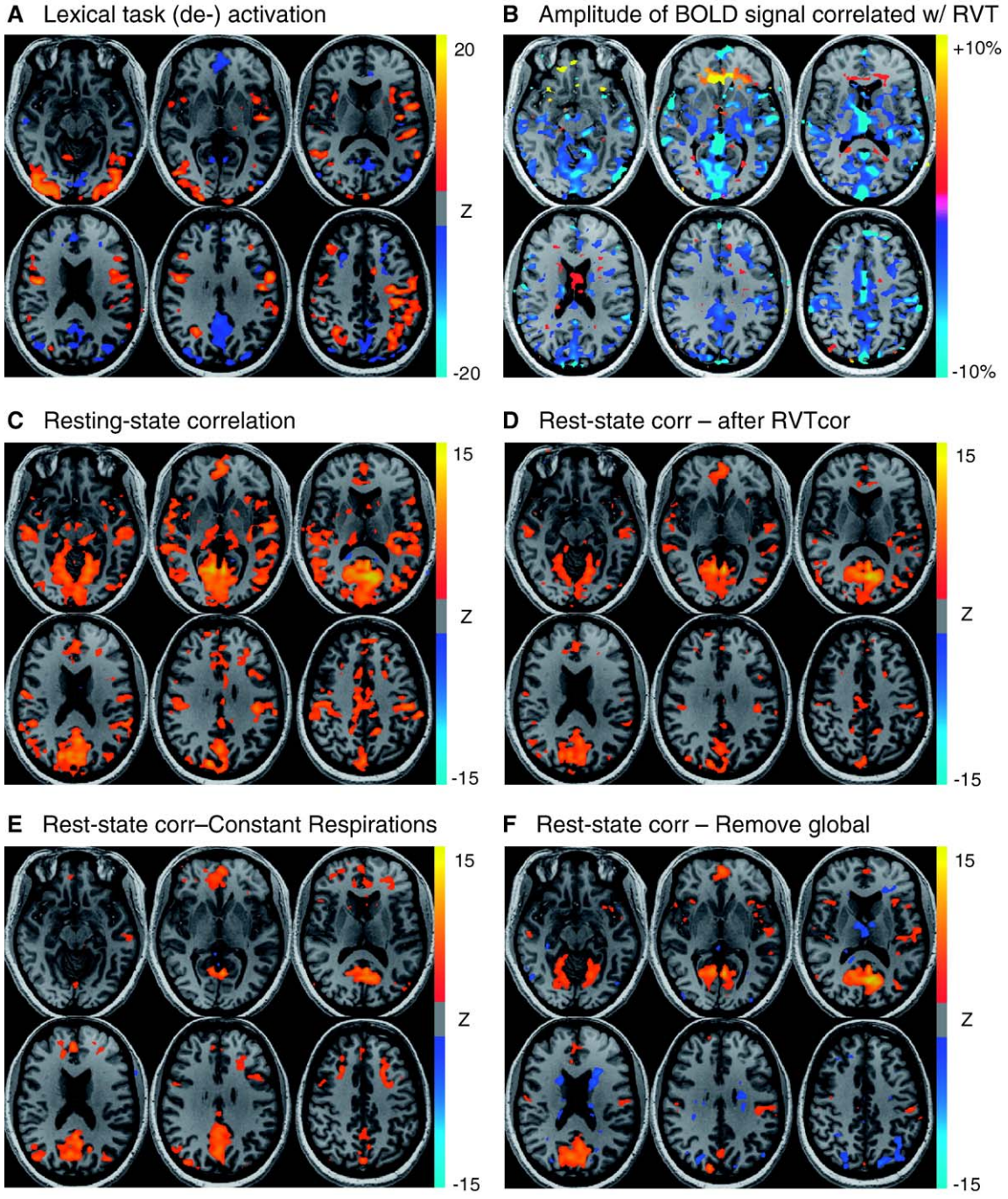

Fig. 6. Maps from a representative subject: (A) activations and deactivations from a lexical task. (B) fMRI signal correlated with respiration volume per time (RVT) changes. (C–F) Functional connectivity map obtained by correlating the average resting signal, before or after correction, from areas in the posterior cingulate that were deactivated in the lexical task. (C) Without any physiological correction. (D) After removing signal changes correlated with respiration volume per time (RVTcor). (E) When subjects were asked to breathe at a constant rate and depth. (F) After global signal changes (averaged over the whole brain) were regressed out.

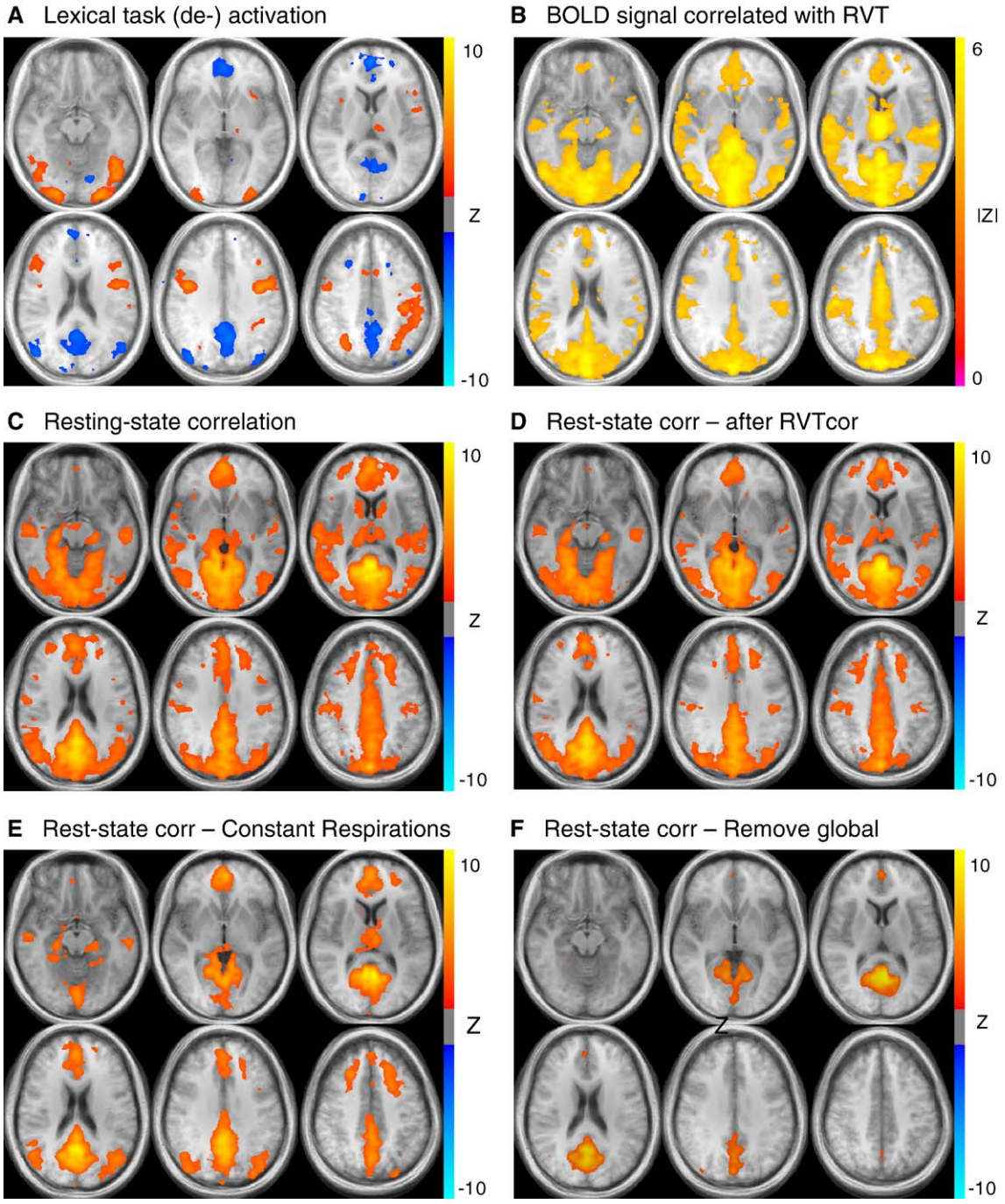

Fig. 7. Group maps: (A) activations and deactivations from a lexical task. (B) fMRI signal correlated with respiration volume per time (RVT) changes. (C–F) Functional connectivity map obtained by correlating the average resting signal, before or after correction, from areas in the posterior cingulate that were deactivated in the lexical task. (C) Without any physiological correction. (D) After removing signal changes correlated with respiration volume per time (RVTcor). (E) When subjects were asked to breathe at a constant rate and depth. (F) After global signal changes (averaged over the whole brain) were regressed out.

decreases in activity during task performance (Cordes et al., 2000; Greicius et al., 2003; Hampson et al., 2002; Kiviniemi et al., 2003; Lowe et al., 1998). The ability to map not only the brain's response to particular tasks but also the differences in the baseline brain state is certainly attractive for a number of mental illnesses. The difficulty with deriving these so-called "functional connectivity" maps is that there are several other physiological fluctuations which may be unrelated to variations in neuronal activity or whose connections to the underlying neuronal activity are unclear. A recent study, for example, has found that the BOLD fMRI signal in certain brain regions is significantly correlated with small variations in end-tidal CO_2 (Wise et al., 2004).

Low-frequency oscillations in arterial and end-tidal levels of CO_2 have commonly been observed during rest and are hypothesized to be due to respiratory feedback mechanisms (Modarreszadeh and Bruce, 1994; Van den Aardweg and Karemaker, 2002).

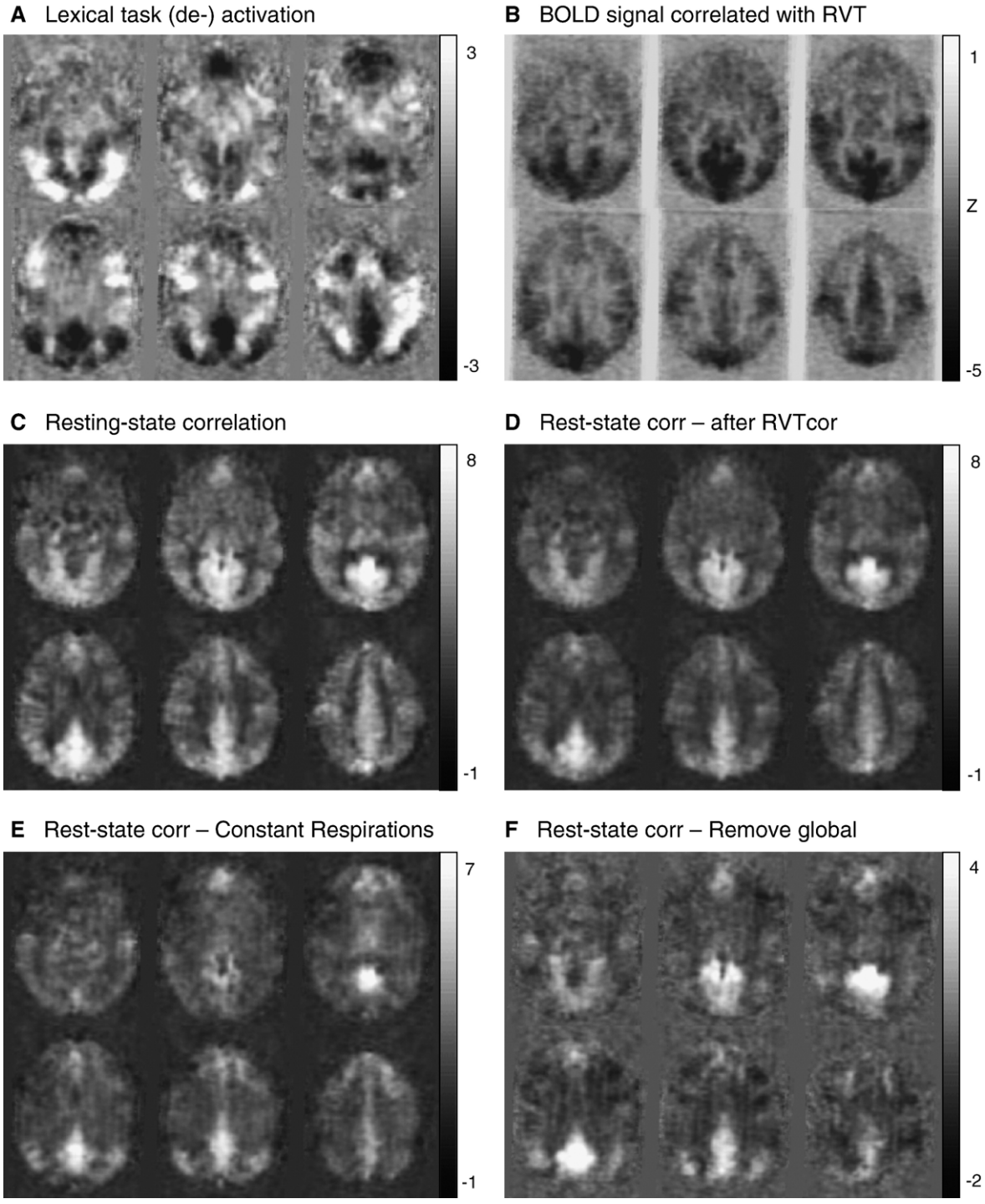

Fig. 8. Unthresholded group maps: *Z* scores of activations, respiration changes, and functional connectivity shown in Fig. 7, without a threshold.

A small change in the rate or depth of breathing causes a variation in the arterial level of CO_2, which is reflected in the measure of end-tidal CO_2 (Robbins et al., 1990). CO_2 is a potent vasodilator, resulting in an increase in cerebral blood flow and hence an increase in the BOLD signal. This increase in response to hypercapnia has been studied extensively in fMRI using both the administration of CO_2 and breath-holding (Bandettini and Wong, 1997; Davis et al., 1998; Kastrup et al., 1999a,b,c; Li et al., 1999; Rostrup et al., 2000; Stillman et al., 1995). Similarly, a decrease in arterial CO_2 results in a decreased CBF and a decreased BOLD signal, as shown by fMRI studies using hyperventilation (Posse et al., 2001). The small fluctuations in arterial CO_2 levels that occur during rest, without an explicit respiratory challenge, therefore lead to fluctuations in the cerebral blood flow and BOLD signal. In addition, the changing levels of CO_2 trigger chemoreflexes that change the depth and rate of subsequent breaths (Modarreszadeh and Bruce, 1994; Van den Aardweg and Karemaker, 2002), thus forming a feedback cycle. The cycle of this chemoreflex-mediated

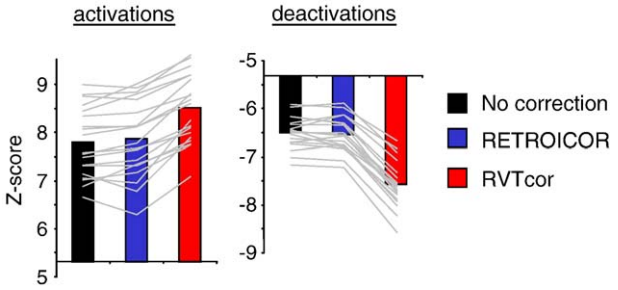

Fig. 9. Detection of (de-)activation: Average Z scores for regions positively ("activations") and negatively ("deactivations") correlated with the lexical task without correction, with RETROICOR correction, and with respiration volume per time correction (RVTcor).

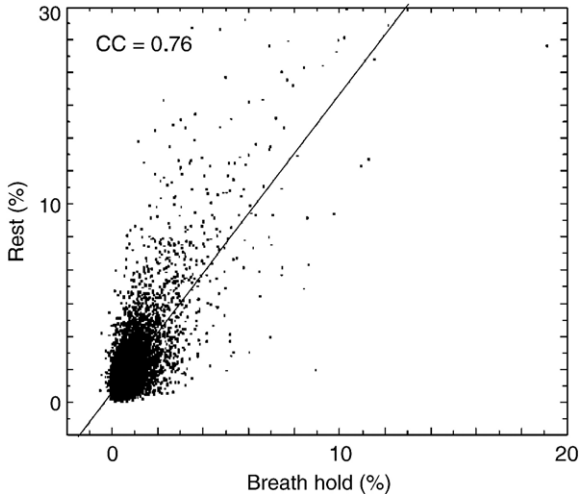

Fig. 11. Comparison to breath-holding: The scatter plot shows the amplitude of signal changes correlated with fluctuations in respiration volume per time (at rest) vs. the amplitude of signal changes correlated with breath-holding for the subject shown in Fig. 10. Each point represents one voxel in the brain. Positive signal changes reflect signal increases in response to decreases in respiration volume. The two amplitudes are correlated with a correlation coefficient of 0.76.

feedback has been measured to be around 25 s or longer, resulting in fluctuations in the range of 0.04 Hz and below.

The hypothesis that changes in CO_2 are responsible for the correlation between respiration changes and fMRI signal fluctuations at rest is supported by the observation that the spatial pattern of these fMRI changes is similar to that observed in response to breath-holding. While there are a number of mechanisms that can cause fMRI signal changes in response to breath-holding, such as intrathoracic pressure changes and CO_2 increases, breath-holding after expiration is most commonly thought to induce BOLD changes via vasodilation resulting from increases in CO_2 (Kastrup et al., 1998, 1999a,b,c; Li et al., 1999; Thomason et al., 2005). The fairly global increases in blood flow (without an increase in cerebral metabolic rate of oxygen) induced by hypercapnia, either by administration of CO_2 or by breath-holding, have been proposed as a potential method for calibrating the BOLD signal across brain regions and across subjects (Bandettini and Wong, 1997; Davis et al., 1998). Calibration of BOLD signal changes using administered CO_2 has, however, not been widely used, possibly due to the additional equipment, setup time, careful monitoring, protocols required, and reduction in SNR from the calibration procedure itself. Breath-holding for calibration has been suggested as an attractive alternative, but this technique is not likely to be viable for many patient populations. The observation in this study that maps of resting variations in respiration are very similar to maps of fMRI signal changes to breath-holding raises the interesting possibility that simple monitoring of subjects respirations during rest, or relatively small manipulations in the depth or rate of breathing, can be used to obtain similar maps for calibration.

From this study, it is not possible to conclusively rule out other mechanisms (in addition to CO_2 mediated blood flow increases) that may be responsible for the correlation between respiration changes and fMRI signal changes. First, a number of brain regions are involved in the control of respiration. These include the ventral

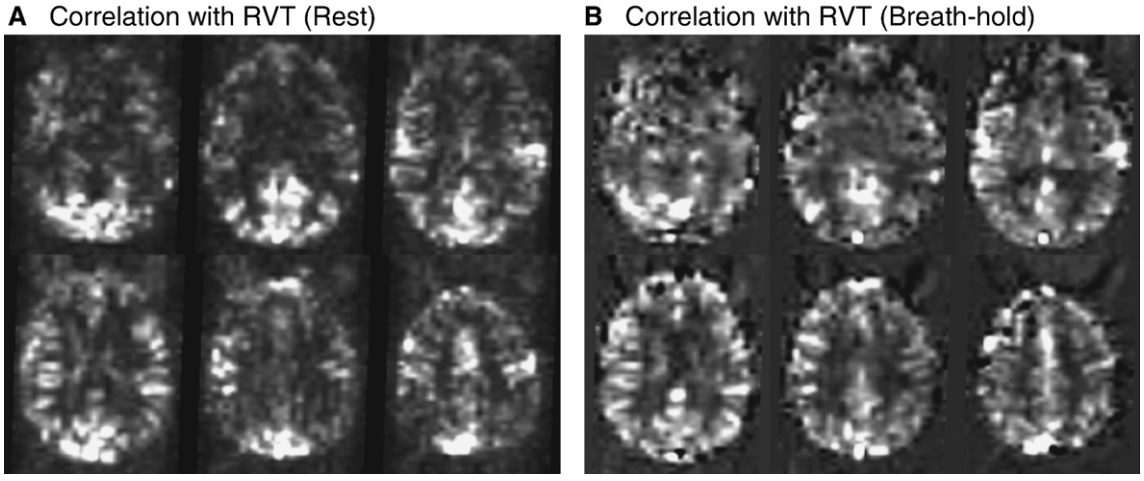

Fig. 10. Comparison to breath-holding: (A) relative amplitude of signal changes correlated with respiration volume per time changes. Scale is reversed—brighter regions correspond to larger decreases in signal correlated with increases in respiration volume per time. (B) Relative amplitude of changes correlated with the global signal (averaged over the whole brain) during a breath-holding task. Again, bright regions show increases in signal in response to breath-holding.

and dorsal medulla, midline pons, ventral cerebellum, and in some cases primary and supplementary motor systems, and have been observed in previous fMRI studies involving the manipulation of breathing (Evans et al., 1999; Gozal et al., 1994). Second, a significant correlation between the respiration volume changes and the fMRI signal was consistently observed at two time lags — with a positive correlation preceding the negative in each voxel by an average of 10.3 s. The simplest explanation of this characteristic is that the correlation of two oscillating signals (in this case, the respiration volume change and the fMRI signal) will result in positive and negative correlations separated by half a period. Alternatively, the positive correlation may reflect the feedback of CO_2 levels in the blood modulating the respirations at a later time. Finally, the similarity between the fMRI signal changes correlated with respiration volume changes and the default mode network is striking. One intriguing possibility is that this may reflect a direct or indirect involvement of the default mode network in the control of respirations. Another possibility is that regions comprising the default mode network have a denser vascular supply which therefore also leads to larger respiration-induced flow changes. An alternative hypothesis is that these regions have such a large blood volume and baseline metabolism that the "default mode network" might simply reflect those regions where BOLD fMRI is most sensitive to any tiny change in blood oxygenation because of the large blood volume. Unfortunately, the possible contribution of these various mechanisms cannot be conclusively determined from this study. A further set of studies needs to be designed specifically to probe the mechanisms of these respiration-related fMRI signal changes and their potentially deeper connection to the default mode network.

Previous studies have found significant correlation between the fMRI signal at rest and the fluctuations in end-tidal CO_2 as measured by a capnograph (Wise et al., 2004). In this study, we measure the depth and rate of respirations using a pneumatic belt placed around the subject's abdomen, reasoning that the changes in end-tidal CO_2 observed in previous studies are primarily related to changes in breathing. This respiration belt is easy to apply, well tolerated by all subjects, uses equipment already supplied by many scanner manufacturers, and is already in routine use for fMRI studies in our group. Previous physiology work has shown a direct relationship between the inspired volume and the end-tidal CO_2 (Guyton, 1986; Van den Aardweg and Karemaker, 2002). Furthermore, the spatial maps of fMRI signal changes correlated with the respiration volume per time derived from this respiration belt look very similar to maps of signal changes observed to be correlated to end-tidal CO_2 in previous studies, and to maps of signal changes correlated with breath-holding, indicating that both are looking at a similar mechanism and that the respiration belt measurement can be used as an approximation of the end-tidal CO_2.

Placing the respiration belt around the abdomen at the level of the diaphragm has produced good respiration measurements in most of our subjects. The use of only a single belt, however, is sensitive to changes in breathing pattern from abdominal to thoracic breathing. If these changes occur within a run, the estimate of the resultant changes in arterial, and consequently end-tidal, CO_2 can be adversely affected. While there is likely a good correlation between the distention of the chest wall and the amount of air inspired, and hence the amount of CO_2 exchanged, the precise temporal shape of the CO_2-induced fMRI signal change may not be fully reflected in the envelope (i.e. peak-to-peak variation) of the respiration belt measurement. For example, a sudden increase in the depth of breathing is likely to result in a slower, not a sudden, decrease in blood flow. As a result, regressing out respiration volume per time changes may not completely remove respiration-induced fMRI signal fluctuations. This might explain the relatively small improvement seen in the functional connectivity analysis when the respiration volume per time changes are regressed out. This can also explain the improved functional connectivity maps when global signal changes are regressed out and the success of using this technique in previous studies of functional connectivity (Fox et al., 2005). Since fMRI signal changes induced by variations in respiration depth and rate occur throughout the brain in gray matter and blood vessels, it is a prominent contributor to the global signal change (the signal change averaged over the whole brain). This global signal, which in fact is shown here to be significantly correlated with the respiration volume per time, may more accurately reflect the temporal shape of respiration-volume-induced fMRI signal changes and therefore lead to improved correction. An inherent danger with regressing out the global signal, however, is that, if the resting-state fluctuations are significant or widespread enough, they will contribute to the global signal. In that case, regressing out the global signal would remove the very signal one is trying to detect. Keeping respiration changes from influencing the data in the first place, by having the subject breathe at a constant rate and depth, results in functional connectivity maps that agree more closely with areas deactivated by the lexical task and do not include areas that were highly correlated with respiration volume per time changes. This may therefore provide a better solution for functional connectivity analysis.

A potential difficulty with cueing the subject to breathe at a constant rate and depth is that this act of controlling respirations may constitute a task and that therefore the functional connectivity may not represent true "resting" correlations. The default mode network has been defined by regions that exhibit decreases in BOLD fMRI signal across a wide range of tasks. Certainly, if a seed voxel time course were chosen from the posterior cingulate during the lexical task, other regions that were similarly deactivated would be highly correlated. The control of respiration, however, was performed throughout the entire run. For this to cause increased correlations within the default mode network, it would require not a general decrease in activity within this network during the entire run, but either a modulation in the control of respiration or fluctuations in the attention to respiration that are synchronous with the depth or rate of breathing. In addition, the standard deviation maps show a marked reduction in the temporal fluctuations in regions correlated with the respiration volume changes. To further rule out this confound, a future study could be designed where subjects are cued to breathe in an irregular manner, with varying rate and depth, similar to what is measured during normal rest.

A number of regions were found to be correlated with the fluctuations in the posterior cingulate at rest, which were not deactivated during the lexical task. Inferring that this discrepancy is due to variations in respiration assumes that the task-related deactivations occur in all the same areas that have correlated resting brain activity. While there is certainly evidence to support the notion that the two reflect similar underlying processes (Greicius et al., 2003), the two need not always be the same. It is possible, for example, that there is a more extensive network of brain regions correlated at rest, only part of which is deactivated during the lexical task. The brain activity during the resting runs

may also involve additional areas that are not as active during the baseline fixation condition of the lexical task. The fact that the subjects' eyes were closed during the resting runs, for example, may have resulted in increased alpha EEG rhythms and additional activations (Goldman et al., 2002). This may also account for the extended BOLD response during the resting condition as compared to the cued constant breathing. A slight correlation between the respiration volume changes and the lexical task was found (CC = 0.3 ± 0.1), raising the additional possibility that the deactivations during the lexical task may in part reflect respiration-related changes. This, however, appears unlikely because the respiration-related changes are generally not as focal as the observed deactivations.

The variability in breathing was generally greater during resting runs than during both lexical and constant breathing runs. This increased variability may be the result of a change in the level of arousal during resting runs where subjects are more likely to be falling asleep. A simple task, such as the lexical decision making task performed here, keeps the subject more aroused. Consequently, the respiration is more steady, similar to cued constant breathing.

FMRI signal changes correlated with variations in respiration volume per time are strongest near large vessels, which typically also show strong cardiac-induced signal fluctuations. Since the TR in this study (2 s) was considerably longer than the cardiac period, one concern is that the low-frequency fluctuations correlated with respiration volume changes may in fact reflect aliased cardiac fluctuations. In this study, cardiac fluctuations were reduced by using a retrospective correction technique, RETROICOR (Glover et al., 2000). In this routine, an external measure of the heart beat (a pulse-oximeter) is used to calculate the phase of the cardiac cycle at which each image was acquired. Variations at this phase and at twice this phase (representing the first harmonic of the cardiac fluctuation) are modeled and regressed out of the time series. Investigations in one subject using higher orders of sinusoids to model higher harmonics did not significantly reduce the residual time series variance. Furthermore, spectral analysis of the cardiac waveforms showed that the peak at around 0.03 Hz did not result from an aliasing of the cardiac peak or its first 2 harmonics.

Correcting for variations in respiration depth and rate by regressing the respiration volume per time out of the time series resulted in a substantial increase in the ability to detect functional activation, as shown in Fig. 9. This improvement was much larger than improvements afforded by conventional physiological corrections. This is most likely due to two reasons. First, the locations of the activations, and in particular the deactivations, occurred in regions most heavily affected by respiration artifacts. Secondly, the BOLD signal changes resulting from the blocked design task with 30-s task periods alternated with 30-s rest periods occurred at a low frequency (0.017 Hz) that overlapped more with the low-frequency variation in the respiration depth and rate. When changes in respiration rate or depth are correlated with the task, regressing out the respiration volume per time, or the global signal, becomes problematic since the BOLD response to the task itself may be removed. In this study, there was a small correlation between the respiration volume per time and the lexical task (CC = 0.3 ± 0.1), but it did not result in a decreased ability to detect task-related BOLD changes. Part of this may be due to a slight difference in the latency between respiration-induced and task-induced BOLD fMRI signal changes. A better understanding of the timing of these respiration induced fMRI signal changes may help in the development of methods to distinguish them from the BOLD response to task-related neuronal activation. Monitoring respirations in these tasks, as well as all functional MRI studies, is vital both for the identification of possible confounds and for the future improvement of correction techniques.

Another analysis tool that can be used to derive maps of functional connectivity is independent components analysis (ICA) (Greicius et al., 2004; Kiviniemi et al., 2003; Kiviniemi et al., 2004). This data-driven approach separates the time course data into several temporally and spatially independent components. Kiviniemi et al. applied this technique to resting-state data and were able to separate out several clusters showing fluctuations at 0.03 Hz, many of which were located in regions defined in other studies to be part of resting-state networks (Kiviniemi et al., 2003). Greicius et al. applied ICA to resting-state data in Alzheimer's patients and consistently found components with fluctuations occurring at low frequencies (<0.1 Hz) matching the spatial profile of the default mode network (Greicius et al., 2004). It is unclear, however, how well ICA can differentiate fMRI signal changes related to variations in respiration from BOLD signal changes induced by activity of the default mode network since these two effects occur in similar regions and at similar frequencies.

Conclusion

Detection of task-related BOLD signal changes is improved when changes in respiration volume per unit time are regressed out of the signal. This improvement was largest in regions with a high density of blood vessels. Including these respiration fluctuations as regressors in the analysis, however, should be done with caution in cases where the breathing pattern is likely to vary in synchrony with the task.

The natural variation in breathing depth and rate during rest has a particularly significant impact on resting-state functional connectivity analysis because the induced fMRI signal changes can occur at similar spatial locations and temporal frequencies. Regressing out variations in the respiration volume per time, as derived from a respiration belt, resulted in only a small reduction of correlated regions outside the default mode network. When global signal changes were regressed out, or when subjects were cued to maintain a constant breathing rate and depth, regions correlated with the posterior cingulate included primarily the regions of the default mode network.

Clearly, improvements in the localization of functional activation and determination of functional connectivity require that the sources of variability in the fMRI data are understood and properly removed or modeled. Monitoring subjects' respirations using a pneumatic respiration belt, a device that is already available on many MR scanners, is easy to implement and does not interfere with most tasks performed in the MR environment. As demonstrated in this study, the benefits of this simple additional step to fMRI experiments can be substantial both for the study of task-related activation and in particular for the analysis of resting-state fMRI data.

Acknowledgment

Support for this research was provided by the National Institute of Mental Health Intramural Research Program.

References

Bandettini, P.A., Wong, E.C., 1997. A hypercapnia-based normalization method for improved spatial localization of human brain activation with fMRI. NMR Biomed. 10 (4–5), 197–203.

Biswal, B., Yetkin, F.Z., Haughton, V.M., Hyde, J.S., 1995. Functional connectivity in the motor cortex of resting human brain using echo-planar MRI. Magn. Reson. Med. 34 (4), 537–541.

Biswal, B., DeYoe, A.E., Hyde, J.S., 1996. Reduction of physiological fluctuations in fMRI using digital filters. Magn. Reson. Med. 35 (1), 107–113.

Chuang, K.H., Chen, J.H., 2001. IMPACT: image-based physiological artifacts estimation and correction technique for functional MRI. Magn. Reson. Med. 46 (2), 344–353.

Cordes, D., Haughton, V.M., Arfanakis, K., Wendt, G.J., Turski, P.A., Moritz, C.H., Quigley, M.A., Meyerand, M.E., 2000. Mapping functionally related regions of brain with functional connectivity MR imaging. AJNR Am. J. Neuroradiol. 21 (9), 1636–1644.

Cox, R.W., 1996. AFNI: software for analysis and visualization of functional magnetic resonance neuroimages. Comput. Biomed. Res. 29 (3), 162–173.

Davis, T.L., Kwong, K.K., Weisskoff, R.M., Rosen, B.R., 1998. Calibrated functional MRI: mapping the dynamics of oxidative metabolism. Proc. Natl. Acad. Sci. U. S. A. 95 (4), 1834–1839.

Evans, K.C., Shea, S.A., Saykin, A.J., 1999. Functional MRI localisation of central nervous system regions associated with volitional inspiration in humans. J. Physiol. 520 Pt 2, 383–392.

Fox, M.D., Snyder, A.Z., Vincent, J.L., Corbetta, M., VanEssen, D.C., Raichle, M.E., 2005. The human brain is intrinsically organized into dynamic, anticorrelated functional networks. Proc. Natl. Acad. Sci. U. S. A. 102 (27), 9673–9678.

Glover, G.H., Li, T.Q., Ress, D., 2000. Image-based method for retrospective correction of physiological motion effects in fMRI: RETROICOR. Magn. Reson. Med. 44 (1), 162–167.

Goldman, R.I., Stern, J.M., Engel, J., Cohen, M.S., 2002. Simultaneous EEG and fMRI of the alpha rhythm. Neuroreport 13 (18), 2487–2492.

Gozal, D., Hathout, G.M., Kirlew, K.A., Tang, H., Woo, M.S., Zhang, J., Lufkin, R.B., Harper, R.M., 1994. Localization of putative neural respiratory regions in the human by functional magnetic resonance imaging. J. Appl. Physiol. 76 (5), 2076–2083.

Greicius, M.D., Krasnow, B., Reiss, A.L., Menon, V., 2003. Functional connectivity in the resting brain: a network analysis of the default mode hypothesis. Proc. Natl. Acad. Sci. U. S. A. 100 (1), 253–258.

Greicius, M.D., Srivastava, G., Reiss, A.L., Menon, V., 2004. Default-mode network activity distinguishes Alzheimer's disease from healthy aging: evidence from functional MRI. Proc. Natl. Acad. Sci. U. S. A. 101 (13), 4637–4642.

Guyton, A.C., 1986. Textbook of Medical Physiology. Saunders, Philadelphia.

Hampson, M., Peterson, B.S., Skudlarski, P., Gatenby, J.C., Gore, J.C., 2002. Detection of functional connectivity using temporal correlations in MR images. Hum. Brain Mapp. 15 (4), 247–262.

Hu, X., Le, T.H., Parrish, T., Erhard, P., 1995. Retrospective estimation and correction of physiological fluctuation in functional MRI. Magn. Reson. Med. 34, 201–212.

Kastrup, A., Li, T.Q., Takahashi, A., Glover, G.H., Moseley, M.E., 1998. Functional magnetic resonance imaging of regional cerebral blood oxygenation changes during breath holding. Stroke 29 (12), 2641–2645.

Kastrup, A., Kruger, G., Glover, G.H., Moseley, M.E., 1999a. Assessment of cerebral oxidative metabolism with breath holding and fMRI. Magn. Reson. Med. 42 (3), 608–611.

Kastrup, A., Kruger, G., Glover, G.H., Neumann-Haefelin, T., Moseley, M.E., 1999b. Regional variability of cerebral blood oxygenation response to hypercapnia. NeuroImage 10 (6), 675–681.

Kastrup, A., Li, T.Q., Glover, G.H., Moseley, M.E., 1999c. Cerebral blood flow-related signal changes during breath-holding. AJNR Am. J. Neuroradiol. 20 (7), 1233–1238.

Kiviniemi, V., Kantola, J.H., Jauhiainen, J., Hyvarinen, A., Tervonen, O., 2003. Independent component analysis of nondeterministic fMRI signal sources. NeuroImage 19 (2 Pt 1), 253–260.

Kiviniemi, V., Kantola, J.H., Jauhiainen, J., Tervonen, O., 2004. Comparison of methods for detecting nondeterministic BOLD fluctuation in fMRI. Magn. Reson. Imaging 22 (2), 197–203.

Li, T.Q., Kastrup, A., Takahashi, A.M., Moseley, M.E., 1999. Functional MRI of human brain during breath holding by BOLD and FAIR techniques. NeuroImage 9 (2), 243–249.

Lowe, M.J., Mock, B.J., Sorenson, J.A., 1998. Functional connectivity in single and multislice echoplanar imaging using resting-state fluctuations. NeuroImage 7 (2), 119–132.

Lund, T.E., Madsen, K.H., Sidaros, K., Luo, W.L., Nichols, T.E., 2006. Non-white noise in fMRI: does modelling have an impact? NeuroImage 29 (1), 54–66.

Modarreszadeh, M., Bruce, E.N., 1994. Ventilatory variability induced by spontaneous variations of $PaCO_2$ in humans. J. Appl. Physiol. 76 (6), 2765–2775.

Posse, S., Kemna, L.J., Elghahwagi, B., Wiese, S., Kiselev, V.G., 2001. Effect of graded hypo- and hypercapnia on fMRI contrast in visual cortex: quantification of T(*)(2) changes by multiecho EPI. Magn. Reson. Med. 46(2), 264–271.

Raichle, M.E., MacLeod, A.M., Snyder, A.Z., Powers, W.J., Gusnard, D.A., Shulman, G.L., 2001. A default mode of brain function. Proc. Natl. Acad Sci. U. S. A. 98 (2), 676–682.

Robbins, P.A., Conway, J., Cunningham, D.A., Khamnei, S., Paterson, D.J., 1990. A comparison of indirect methods for continuous estimation of arterial PCO_2 in men. J Appl. Physiol. 68 (4), 1727–1731.

Rostrup, E., Law, I., Blinkenberg, M., Larsson, H.B., Born, A.P., Holm, S., Paulson, O.B., 2000. Regional differences in the CBF and BOLD responses to hypercapnia: a combined PET and fMRI study. NeuroImage 11 (2), 87–97.

Stillman, A.E., Hu, X., Jerosch-Herold, M., 1995. Functional MRI of brain during breath holding at 4 T. Magn. Reson. Imaging 13 (6), 893–897.

Thomason, M.E., Burrows, B.E., Gabrieli, J.D., Glover, G.H., 2005. Breath holding reveals differences in fMRI BOLD signal in children and adults. NeuroImage 25 (3), 824–837.

Van den Aardweg, J.G., Karemaker, J.M., 2002. Influence of chemoreflexes on respiratory variability in healthy subjects. Am. J. Respir. Crit. Care Med. 165 (8), 1041–1047.

Wise, R.G., Ide, K., Poulin, M.J., Tracey, I., 2004. Resting fluctuations in arterial carbon dioxide induce significant low frequency variations in BOLD signal. NeuroImage 21 (4), 1652–1664.